

Article

Isolation and Identification of Flavonoids from Black Cumin (*Nigella sativa*) by HPLC-MS and In Silico Molecular Interactions of Their Major Compounds with *Fusarium oxysporum* Trypsin-like Serine Protease

Hossam S. El-Beltagi ^{1,2,*}, Seham M. S. Abdel Aziz ³, A. I. Aboshady ³, Mervat A. R. Ibrahim ³, Mohamed F. M. Ibrahim ^{4,*}, Muneefah Abdullah Alenezi ⁵, Doaa Bahaa Eldin Darwish ^{5,6}, Salem Mesfir Al-Qahtani ⁷, Nadi Awad Al-Harbi ⁷, Hadeer Darwish ^{8,9} and Hany A. M. Srour ³

¹ Agricultural Biotechnology Department, College of Agriculture and Food Sciences, King Faisal University, Al-Ahsa 31982, Saudi Arabia

² Biochemistry Department, Faculty of Agriculture, Cairo University, Giza 12613, Egypt

³ Biochemistry Department, Faculty of Agriculture, Ain Shams University, Cairo 11566, Egypt; sehamohamedsamy@yahoo.com (S.M.S.A.A.); ahmed_shadi@agr.asu.edu.eg (A.I.A.); mervat_ibrahim@agr.asu.edu.eg (M.A.R.I.); hany_srour@agr.asu.edu.eg (H.A.M.S.)

⁴ Department of Agricultural Botany, Faculty of Agriculture, Ain Shams University, Cairo 11566, Egypt

⁵ Department of Biology, Faculty of Science, University of Tabuk, Tabuk 71491, Saudi Arabia; makalenezi@ut.edu.sa (M.A.A.); ddarwish@ut.edu.sa (D.B.E.D.)

⁶ Botany Department, Faculty of Science, Mansoura University, Mansoura 35511, Egypt

⁷ Biology Department, University College of Tayma, University of Tabuk, Tabuk 71491, Saudi Arabia; salghtani@ut.edu.sa (S.M.A.-Q.); nalharbi@ut.edu.sa (N.A.A.-H.)

⁸ Department of Biotechnology, College of Science, Taif University, Taif 21944, Saudi Arabia; hadeer@tu.edu.sa

⁹ Department of Medicinal and Aromatic Plants, Horticulture Research Institute, Agricultural Research Center, Giza 12619, Egypt

* Correspondence: helbeltagi@kfu.edu.sa (H.S.E.-B.); ibrahim_mfm@agr.asu.edu.eg (M.F.M.I.)



Citation: El-Beltagi, H.S.; Aziz, S.M.S.A.; Aboshady, A.I.; Ibrahim, M.A.R.; Ibrahim, M.F.M.; Alenezi, M.A.; Darwish, D.B.E.; Al-Qahtani, S.M.; Al-Harbi, N.A.; Darwish, H.; et al. Isolation and Identification of Flavonoids from Black Cumin (*Nigella sativa*) by HPLC-MS and In Silico Molecular Interactions of Their Major Compounds with *Fusarium oxysporum* Trypsin-like Serine Protease. *Separations* **2023**, *10*, 360. <https://doi.org/10.3390/separations10060360>

Academic Editor: Paraskevas D. Tzanavaras

Received: 20 May 2023

Revised: 12 June 2023

Accepted: 15 June 2023

Published: 17 June 2023



Copyright: © 2023 by the authors. Licensee MDPI, Basel, Switzerland. This article is an open access article distributed under the terms and conditions of the Creative Commons Attribution (CC BY) license (<https://creativecommons.org/licenses/by/4.0/>).

Abstract: *Fusarium oxysporum* is one of the most harmful soil-borne pathogens that cause root rot, damping-off, and wilt disease in many plant species. Management of *Fusarium oxysporum* diseases is often by using many harmful and expensive chemical fungicides which have many harmful effects on the environment and human health. The current study was conducted to identify the chemical constituents of black cumin seeds' methanolic extract and investigate the ability of the major constituents to inhibit the *Fusarium oxysporum* trypsin-like serine protease, which play an important role in *F. oxysporum* pathogenicity. The HPLC-MS analysis of black cumin seeds' methanolic extract revealed the presence of seven major compounds: amentoflavone, Procyanidin C2, Quercetin3-O-sophoroside-7-O-rhamnoside, 5,7-Dihydroxy-3,4-dimethoxyflavone, Borapetoside A, tetrahydroxy-urs-12-en-28-O-[*b*-D-glucopyranosyl (1-2)-*b*-D-glucopyranosyl] ester, and kudzusaponogenol A-hexA-pen. The results of molecular docking between these compounds and the active site of *Fusarium oxysporum* trypsin showed that only four compounds were able to bind to the active site of *F. oxysporum* trypsin. Amentoflavone, 5,7-Dihydroxy-3,4-dimethoxyflavone, and Quercetin3-O-sophoroside-7-O-rhamnoside have the highest binding energy, −6.4, −6.5, and −6.5 Kcal/mol, respectively. In addition, the results clarify that 5,7-Dihydroxy-3,4-dimethoxyflavone was the only compound to form a hydrogen bond with Asp189 (the residue responsible for substrate specificity). The results of the study strongly indicate that flavonoids of black cumin seeds' methanolic extract could be used as effective inhibitors for the *F. oxysporum* trypsin-like serine protease.

Keywords: flavonoids; molecular docking; phytopathogenic fungi; plant extracts; serine protease

1. Introduction

Fusarium oxysporum is one of the main pathogens that cause serious damage to numerous monetarily significant crops worldwide. Phytopathogenic fungi including *Fusarium oxysporum* possess a number of extracellular cell-wall-degrading enzymes such as cellulases, pectic enzymes, and proteases; those enzymes cause a lot of damage to plant cell walls during pathogenesis [1,2]. Proteases are important for the pathogenicity and growth of phytopathogenic fungi. Among the proteases that are secreted by phytopathogenic fungi is the trypsin-like serine protease [2]; the serine protease takes its name from the serine residue in its catalytic site. The hydroxyl group of the serine residue is responsible for the first step in peptide bond hydrolysis through acting as a nucleophile [3]. The *F. oxysporum* trypsin-like serine protease consists of two domains; each domain consists of six beta strands. The active site of the *F. oxysporum* trypsin-like enzyme consists of a catalytic site located in the cleft between the two domains and the specificity bucket that is located near the catalytic site serine residue [4]. Until now, the main method for controlling *F. oxysporum* worldwide is chemical fungicides. With the increasing awareness of the damage caused by chemical fungicides to the environment, for instance, affecting non-target organisms and soil micro-organisms and contaminating water sources, in addition to the decrease in their effect on phytopathogenic fungi as a result of the development of resistant strains, the search for other means to control phytopathogenic fungi including *F. oxysporum* has become urgent. One of the possible methods for controlling phytopathogenic fungi is the use of natural compounds. Several studies were conducted to investigate the ability of different natural compounds and plant extracts to inhibit cell-wall-degrading enzymes including proteases as a key role in phytopathogenic fungi control [5,6]. Previous studies have reported the inhibitory effect of black cumin seeds' (*N. sativa*) oil and extracts on phytopathogenic fungi growth. It has been reported that black cumin seeds' oil decreased 56.67% of the severity of root rot disease caused by *Rhizoctonia solani* at a concentration of 5% [7], and the different extracts of black cumin seed can inhibit 76–100% of *Fusarium oxysporum* growth at a concentration of 50 mg/mL [8].

Nigella sativa, commonly known as black cumin (family: Ranunculaceae), is native to south Asia. Black cumin seeds contain a large variety of compounds such as fatty acids, alkaloids, saponins, flavonoids, terpenoids, and quinones [9]. Previous studies showed that black cumin seeds' oil contains high percentage of unsaturated fatty acids, and the major fatty acid was linoleic acid [10]. Moreover, previous studies reported the presence of phenolic compounds including coumaroyl acid derivative and thermoquinol glucoside, flavonoids including quercetin and apigenin, alkaloids including norargemonine and nigellimine, 2-(4-Nitrobutyryl), and saponins such as alpha-hederin, a triterpene saponin in black cumin seeds' extracts [9,11]. Black cumin seeds have been widely used in traditional medicine in the Middle East [12]. In addition, black cumin seeds have been reported to have antibacterial, antifungal, and antioxidant properties [8,13,14].

Recently, several studies have demonstrated that black cumin seeds have an inhibitory effect on different types of proteases including the phytopathogenic fungi *R. solani* extracellular protease. It has been reported that black cumin seeds' methanolic extract at 2000 ppm inhibited 74% of *R. solani* protease activity [15]. Moreover, it has been reported that black cumin seeds' oil inhibited 75.4% and 91.1% of the serine protease elastase type I and type II activity, respectively, and 92.4% of collagenase activity at a concentration of 300 µg/mL [16]. On the other hand, there is no available information about the effect of black cumin seeds on the extracellular trypsin-like protease of *F. oxysporum*.

Molecular docking is a tool used widely in drug discovery studies; it based on using software to predict the interaction between a known 3D structure of a target protein and a small molecule (ligand) and the most likely binding conformation of the ligands and its binding affinity through thermodynamic favorability [17]. The aims of this study are to identify the chemical composition of black cumin seeds' (*N. sativa*) methanolic extract and to clarify the ability of the major chemical constituents to bind and inhibit the trypsin-like serine protease from *Fusarium oxysporum* using molecular docking methods.

2. Results and Discussion

2.1. Analysis of Black Cumin Seeds' Methanolic Extract by HPLC-MS

The yield of the extraction was 30% (*w/w*). Forty-three peaks resulted from the HPLC-MS analysis of black cumin seeds' methanolic extract (Figure 1). Seventeen peaks were identified and presented in Table 1, whereas the rest of the peaks were considered to be unknown. The identified peaks represent 83% of the peaks' area. Table 1 shows the retention time, *m/z* for the $[M-H]^-$ ion, *m/z* of the ESI-MS fragments, chemical formula, and the percentages of identified peaks.

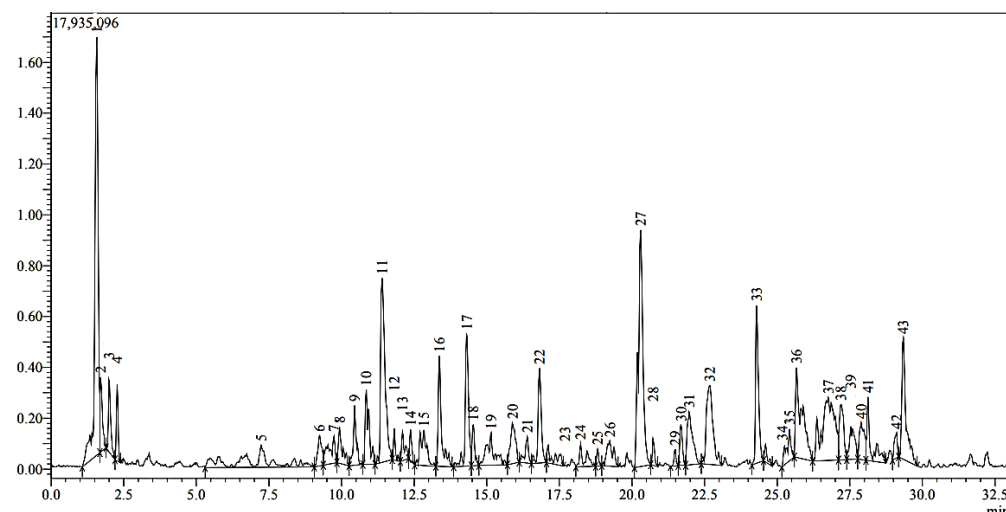


Figure 1. MS chromatogram of black cumin seeds' methanolic extract.

Peaks 1, 4, 7, 10, 11, 12, 27, and 33 were identified as flavonoids or flavonoid glycosides. Peak 1, 10, and 27 were previously identified as amentoflavone, quercetin-3-O-sophoroside-7-O-rhamnoside, and procyanidin C2, respectively (Figure 2) [15,18–20]. The mass spectrum of peak 4 showed the $[M-H]^-$ ion at 237 *m/z* in addition to the base peak ion $[M-H-H_2-CO_2]^-$ at 191 *m/z* and $[M-H-H_2-B^{14}]^-$ ion at 128 *m/z*, resulting from the loss of H_2 and the cleavage of bonds 1 and 4 in ring C. In comparison with the fragmentation pattern of flavones from the literature [21,22], peak 4 (*t_R* = 2.28 min) was identified as hydroxyflavone (Figure 2). Peak 7 (*t_{R = 9.74 min) produced the $[M-H]^-$ ion at 779 *m/z*, with the $[M-H-170]^-$ ion at 609 *m/z* indicating the loss of dehydroxyshikimic acid and the base peak ion $[M-H-170-146-18-120]^-$ at 327 *m/z*, resulting from the loss of dehydroxyshikimic followed by the loss of the pentose moiety, H_2O , and ${}^{0,3}X$ fragment of the hexose moiety. Comparing the fragmentation pattern of peak 7 with the literature [23–25], peak 7 was identified as Quercetin 3-O-dehydroxy shikimic acid-rhamnosyl-(1→4)-glucoside (Figure 2). Peak 10 (*t_{R = 10.85 min) gave the $[M-H]^-$ ion at 917 *m/z* and $[M-H-486]^-$ ion at 431 *m/z*, resulting from the loss of dehexose coumaroyl and O-hexose. Peak 10 was identified as flavonol base + 4O, O-dHex-Hex-Hex-Coumaroyl [20]. Peak 12 (*t_{R = 11.82 min) generated the $[M-H]^-$ ion at 607 *m/z*, with the base peak ion $[M-H-146]^-$ at 461 *m/z*, resulting from the loss of dehexose, the $[M-H-146-46]^-$ ion at 415 *m/z*, and $[M-H-146-162-31-B^{14}]^-$ at 149 *m/z*, resulting from the loss of the dehexose and hexose moieties, OCH_3 , and the cleavage of bonds 1 and 4 in ring C of diosmetin. According to the fragmentation pattern of peak 12, it was identified as diosmetin 7-neohesperidoside (Figure 2) [26].}*}*}*

Table 1. HPLC-MS analysis of methanolic extract of black cumin seeds (*N. sativa*).

Peak	tR (min)	[M-H] ⁻ (m/z)	ESI-MS (m/z)	Formula	Identification	% Area
1	1.57	537	387, 357, 195	C ₃₀ H ₁₈ O ₁₀	Amentoflavone	36.8
4	2.28	237	191, 128	C ₁₅ H ₁₀ O ₃	Hydroxyflavone	0.6
7	9.74	779	609, 497, 327, 171	C ₃₄ H ₃₆ O ₂₁	Quercetin 3-O-dehydroxy shikimic acid-rhamnosyl-(1)- 4→glucoside	0.3
8	9.93	325	266, 175, 137	C ₁₅ H ₁₈ O ₈	Thermoquinol glucoside	0.3
9	10.45	933	535, 489, 239	C ₄₁ H ₂₆ O ₂₆	castalagin	0.6
10	10.85	917	431	C ₄₂ H ₄₆ O ₂₃	Flavonol base + 4O, O-dHex-Hex-Hex-Coumaroyl	1.4
11	11.4	771		C ₃₃ H ₄₀ O ₂₁	Quercetin3-O-sophoroside-7-O- rhamnoside	9.9
12	11.82	607	543, 461, 415, 149	C ₂₈ H ₃₂ O ₁₅	Diosmetin 7-neohesperidoside	0.1
13	12.1	765	439, 407, 371, 321, 233	C ₄₁ H ₆₆ O ₁₃	Soyasaponin IV	0.2
16	13.37	797	675, 629	C ₄₁ H ₆₅ O ₁₅	Kudzusapogenol A-hexA-pen	2.4
17	14.31	827	413	C ₄₂ H ₆₇ O ₁₆	Tetrahydroxy-urs-12-en-28-O-[b-D-glucopyranosyl (1-2)-b-D-glucopyranosyl] ester	3.2
18	14.53	187		C ₁₁ H ₈ O ₃	Plumbagin	0.3
22	16.82	791	395		Oleanoic acid-hex A-pent	1.8
27	20.29	865	525, 251	C ₄₅ H ₃₈ O ₁₈	Procyanidin C2	16.7
33	24.29	313	245	C ₁₇ H ₁₄ O ₆	5,7-Dihydroxy-3,4-dimethoxyflavone	4.5
42	29.1	555	393, 327, 295	C ₂₆ H ₃₆ O ₁₃	Tinosineside A	0.1
43	29.34	537	341, 295	C ₂₆ H ₃₄ O ₁₂	Borapetoside A	4.1
Total						83.3

Peak 33 (tR = 24.29 min) produced the [M-H]⁻ ion at 313 m/z and [M-H-68]⁻ ion resulted from the neutral loss of C₃O₂ at 245 m/z (Figure 3). In comparison with the fragmentation pattern of flavanones from the literature [20], peak 33 was identified as 5,7-dihydroxy-3,4-dimethoxyflavone.

Peaks 13, 16, 17, and 22 were identified as triterpenoids glycosides. Peak 13 (tR = 12.1 min) produced the [M-H]⁻ ion at 765 m/z, with the [M-H-132-176-18]⁻ ion at 439 m/z, resulting from the loss of pentose (132 Da), glucuronic acid (176 Da), and the water molecule, [agly-H-18-32]⁻ at 407 m/z corresponding to the loss of the water molecule and the methanol molecule from the aglycone, and the base peak ion [agly-H-18-32-18-18]⁻ at 371 m/z corresponding to loss of another two water molecules from the aglycone. Peak 16 (tR = 13.37 min) gave the [M-H]⁻ ion at 797 m/z, with the base peak ion [M-H-18-44-60]⁻ ion at 675 m/z, corresponding to the loss of the water molecule and COO from the glucuronic acid moiety and ^{0,4}X fragment of the pentose moiety (Figure 3). By comparing the fragmentation pattern of peaks 13 and 16 with the literature [27], peaks 13 and 16 were identified as soyasaponin IV and kudzusapogenol A-hexA-pen, respectively. Peak 17 (tR = 14.31 min) generated two ions, the [M-H]⁻ ion at 827 m/z and the base peak ion [M-H-414]⁻ ion at 413 m/z corresponding to the loss of two hexose moieties and COO (44 Da), H₂O (18 Da), and CO (28 Da) from the aglycone (Figure 3). Peak 17 was identified as the tetrahydroxy-urs-12-en-28-O-[b-D-glucopyranosyl (1-2)-b-D-glucopyranosyl] ester [28]. Similar to peak 17, peak 22 (tR = 16.82 min) produced two ions, the [M-H]⁻ ion at 791 m/z and the base peak ion [M-H-396]⁻ ion at 395 m/z, corresponding to the loss of

glucuronic acid (176 Da) and the hexose moiety (162 Da), and COO and CH₂ (14 Da) from the aglycone. By comparing the fragmentation pattern of peak 22 with the literature [29], peak 22 was identified as oleanoic acid-hex A-pent.

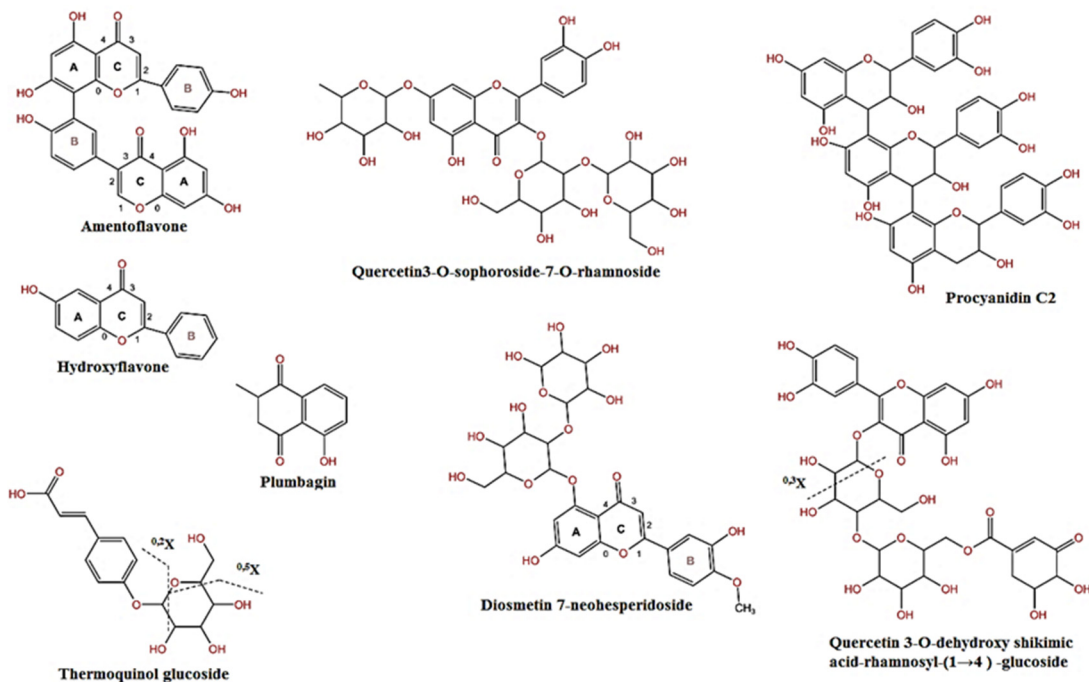
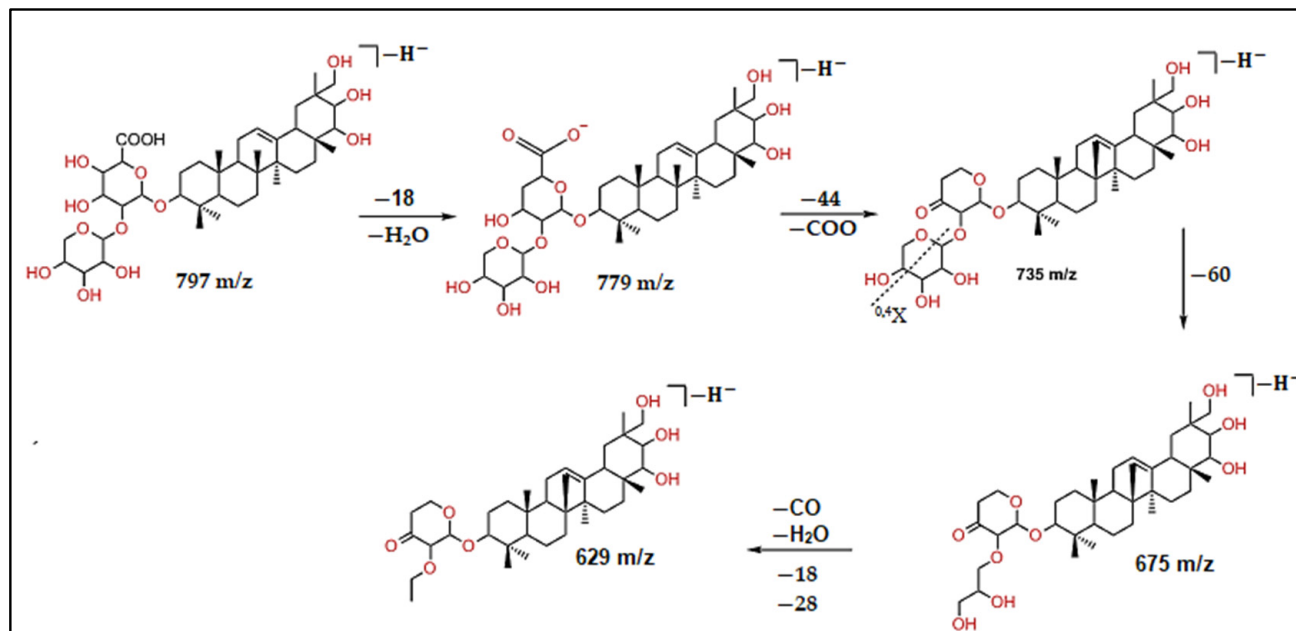


Figure 2. Chemical structure of the compounds identified in black cumin seeds' methanolic extract.



(a)

Figure 3. Cont.

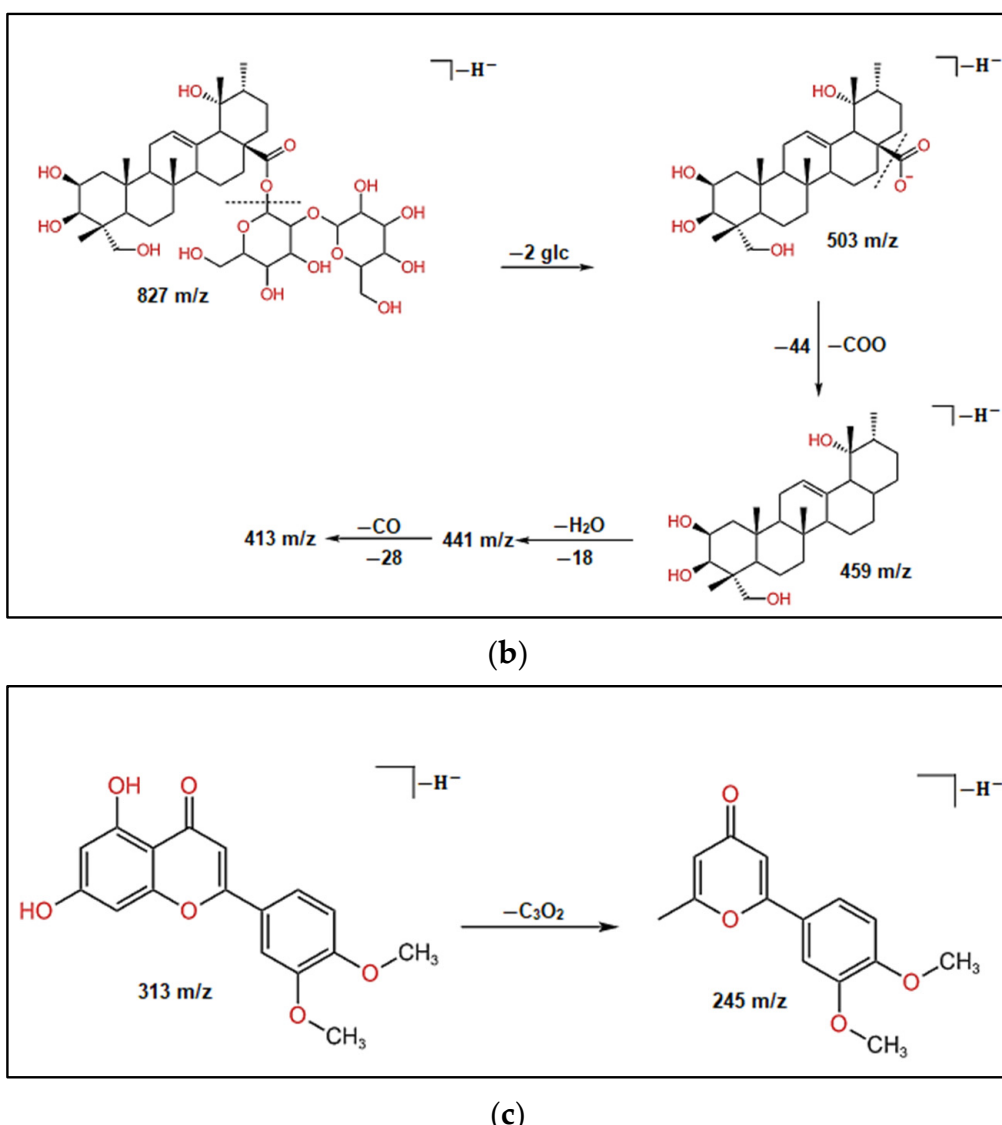


Figure 3. Fragmentation patterns of (a) peak 16; (b) peak 17; and (c) peak 33.

Peaks 42 and 43 were assigned to be diterpenoids glycosides. Peak 42 ($tR = 29.1$ min) gave the $[M-H-162]^-$ ion at $393\text{ }m/z$ corresponding to the loss of hexose, $[M-H-162-18-18-30]^-$ ion at $327\text{ }m/z$ corresponding to loss of hexose, 2 H_2O , and $2CH_3$, and the base peak ion $[M-H-180-18-18-44]^-$ at $295\text{ }m/z$ corresponding to loss of O-hexose, 2 H_2O , and COO . Similar to peak 42, peak 43 ($tR = 29.34$ min) gave the base peak ion $[M-H-180-18-44]^-$ at $295\text{ }m/z$ and $[M-H-180-18]^-$ at $441\text{ }m/z$ (Figure 4). The $[M-H]^-$ ion of peaks 42 and 43 were absent. Peaks 42 and 43 were identified as tinosineside A and borapetoside A, respectively [30].

Peak 8 ($tR = 9.93$ min) produced its $[M-H]^-$ ion at $325\text{ }m/z$, $[M-H-60]^-$ ion at $266\text{ }m/z$, and $[M-H-150]^-$ ion at $175\text{ }m/z$, indicating the presence of fragments $^{0.5}X$ and $^{0.2}X$ of the hexose moiety, respectively, and the base peak ion $[M-H-162-26]^-$ at $137\text{ }m/z$ corresponding to loss of hexose and $2CH$. In comparison with the fragmentation pattern from previous studies [31], peak 8 was identified as thymoquinol glucoside (Figure 2).

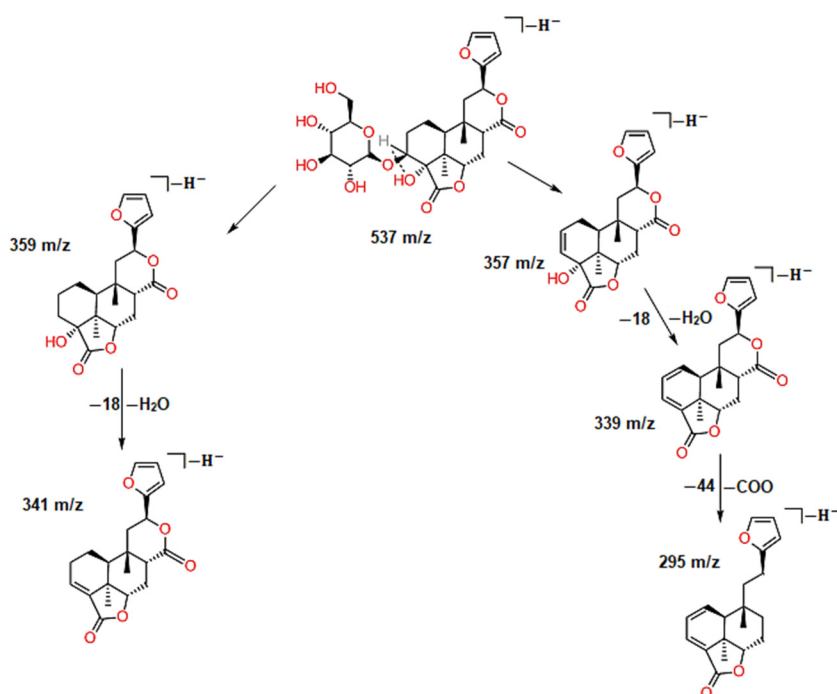


Figure 4. Fragmentation pattern of peak 43.

Peak 9 ($t_{R} = 10.45$ min) generated its $[M-H]^-$ and base peak ion at $933\text{ }m/z$ and $[M-H-694]^-$ ion at $239\text{ }m/z$, resulting from a lactonization reaction which resulted in the formation of the [ellagic acid-H] $^-$ ion (301 Da) and [castalin-H] $^-$ ion. The loss of CO_2 and H_2O from the [ellagic acid-H] $^-$ ion produced the peak at $239\text{ }m/z$. Peak 9 was identified as castalagin [31]. Peak 18 ($t_{R} = 14.53$ min) gave its $[M-H]^-$ and only peak at $187\text{ }m/z$. Peak 18 was identified as plumbagin (Figure 2) [32].

Peak 18 gave its $[M-H]^-$ and only peak at $187\text{ }m/z$. In comparison with the literature [33], peak 18 was identified as plumbagin (Figure 2).

2.2. Molecular Docking Analysis

AutoDock Vina 1.2.0 was used for a docking study of eight compounds from black cumin seeds' methanolic extract and the known serine protease inhibitor benzamidine against the active site of the *Fusarium oxysporum* trypsin-like serine protease. The active site of the *F. oxysporum* trypsin consists of the catalytic site (His57, Ser195, and Asp102) and the specificity pocket S1 (Asp189, Gly216, Asn217, Gly219, and Ser225) [4].

To validate the obtained results of the AutoDock Vina protocol, we have re-docked the substrate that consists of single peptide GLY-ALA-LYS into the enzyme active site and compared the interaction with the X-ray structure of the *F. oxysporum* trypsin enzyme and substrate complex (1GDN). The result showed that the substrate binds to the active site of the enzyme with a conformation very similar to the conformation reported in the X-ray structure (Figure 5). In addition to forming all the hydrogen bonds reported in the X-ray structure (Figure 5), Lys formed two hydrogen bonds with Ser190 and Gly193, Ala formed one hydrogen bond with Ser214, and Gly formed two hydrogen bonds with Gly216. The interactions between Lys and Asp189, His57, and Ser195 (water bridges) that are reported by Rypniewski et al. [4] in the X-ray structure were not possible within the docking method used in the current study. In the current study, the water molecules were deleted before the docking due to the limitation of AutoDock Vina in differentiating between the water atoms and the target protein atoms and treating the target protein atoms and the mediating water molecules as a one rigid structure which causes the water molecules to prevent the binding of the ligands.

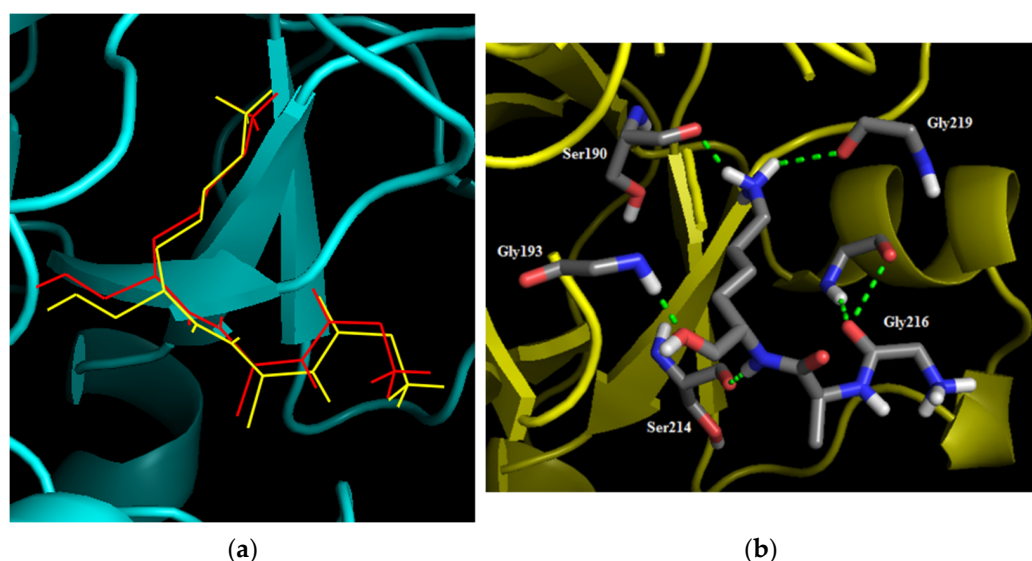


Figure 5. (a) The conformation of substrate in the enzyme active site, the substrate of X-ray structure in red lines, the docked substrate in yellow lines, and the enzyme in cartoon; (b) 3D interactions between the docked substrate and residues in active site of enzyme. Hydrogen bonds in green dashes, the interacted residues and ligands in gray sticks, and the enzyme in cartoon.

Three compounds showed no affinity toward the active site of the *F. oxysporum* trypsin-like serine protease, Kudzusapongenol A-hexA-pen, tetrahydroxy-urs-12-en-28-O-[β -D-glucopyranosyl (1-2)- β -D-glucopyranosyl] ester, and procyanidin C2, as demonstrated by the positive binding energy, whereas the rest of the studied compounds were successfully docked to the enzyme. Table 2 shows the binding energy, type of bonds, bonds length, interacted residues, and 2D interactions between the compounds and the *F. oxysporum* trypsin-like serine protease. Amentoflavone, 5,7-dihydroxy-3,4-dimethoxyflavone, and quercetin3-O-sophoroside-7-O-rhamnoside showed the highest affinity toward the enzyme active site with a binding energy of -6.4 , -6.5 , and -6.5 Kcal/mol, respectively. Benzamidine and Borapetoside A bind to the active site of the enzyme with a binding energy of -5.5 and -4.2 Kcal/mol, respectively. All the compounds formed hydrogen bonds with the residues in the enzyme active site except for plumbigan, which binds to the enzyme active site through van der Waals forces only with a binding energy of 5.3 Kcal/mol. Amentoflavone formed two hydrogen bonds with His57 and Gly216, one carbon hydrogen bond with Asn217, and van der Waals forces with Ser195 and Gly219 in the active site of the enzyme and hydrophobic interaction (Pi–Pi stacked) with one residue outside the active site of the enzyme Trp215 (Figure 6), whereas 5,7-dihydroxy-3,4-dimethoxyflavone binds to the active site of the enzyme via two hydrogen bonds with Ser195 and one hydrogen bond with Asp189 and van der Waals forces with Gly216, Gly219, and His57 and binds with two residues outside the active site Glu146 through a carbon hydrogen bond and Trp215 through hydrophobic interactions (Amid–Pi stacked) (Figure 6). Quercetin3-O-sophoroside-7-O-rhamnoside formed one hydrogen bond with Ser195, Pi–donor hydrogen bond with His57, and van der Waals forces with Asn217 in the active site of the enzyme while it formed hydrogen bonds with two residues outside the active site Ser214 and Asn99 and had a hydrophobic interaction (Pi–Pi stacked) with Trp215 (Figure 6). Benzamidine formed two hydrogen bonds, one with Asp189 in the specificity bucket and one with Ser190 outside the active site and salt bridge with Asp189 (Figure 7).

Table 2. Interactions between *Fusarium oxysporum* trypsin-like serine protease and inhibitors.

Inhibitor	2D Interactions	Type of Bonds	Interacted Residues	Bond Length (Å)	BE (Kcal/mol)
Amentoflavone		Hydrogen bonds Carbon hydrogen bonds	His57 Gly216 Asn217	2.52 2.5 3.37	-6.4
Benzamidine		Hydrogen bonds	Asp189 Ser190	2.13 2.05	-5.5
5,7-Dihydroxy-3,4-dimethoxyflavone		Hydrogen bonds Carbon hydrogen bond Amid-Pi stacked	Ser195 Asp189 Glu146 Trp215 (2)	3.18 3.02 3.5 3.64 8.08	-6.5

Table 2. Cont.

Inhibitor	2D Interactions	Type of Bonds	Interacted Residues	Bond Length (Å)	BE (Kcal/mol)
Borapetoside A		Hydrogen bond	Asn99	2.91	
			Gly216 (2)	2.66 2.84	
		Carbon hydrogen bond	Trp41	3.63	
		Pi-Pi T shaped	His57	5.07	-4.2
Plumbagin		Pi alkyl	Cys42	5.08	
					-5.3
Quercetin3-O-sophoroside-7-O-rhamnoside		hydrogen bonds	Gln192 (5)	2.92 2.9 2.99 2.89 2.4	
			Ser214	2.67	
			Asn99	2.43	
			Ser195	2.85	
		Pi-donor hydrogen bonds	His57	2.43	-6.5
		Pi-Pi stacked	Trp215	5.63	

Interactions

- [Green square] Conventional Hydrogen Bond
- [Yellow square] Pi-Donor Hydrogen Bond
- [Blue square] van der Waals
- [Orange square] Salt Bridge
- [Pink square] Pi-Pi T-shaped , Amide-Pi Stacked
- [Dark Blue square] Carbon Hydrogen Bond
- [Light Blue square] Pi-Alkyl
- [Red square] Unfavorable Acceptor-Acceptor

Benzamidine and 5,7-dihydroxy-3,4-dimethoxyflavone were the only compounds that formed hydrogen bonds with the Asp189 residue which consider the residue responsible for the substrate binding and the specificity of the enzyme for the amino acids with a positively charged side chain. Quercetin3-O-sophoroside-7-O-rhamnoside and 5,7-dihydroxy-3,4-dimethoxyflavone were the only compounds that formed hydrogen bonds with the Ser195 residue in the catalytic site of the enzyme; Ser195 is the residue responsible for starting the cleavage of the peptide bond through a nucleophilic attack on the carbonyl group carbon. The results of the docking indicate that flavonoids of black cumin seeds' methanolic extract, amentoflavone, 5,7-dihydroxy-3,4-dimethoxyflavone, and quercetin3-O-sophoroside-7-O-rhamnoside could be effective inhibitors for the *F. oxysporum* trypsin-like serine protease, specially 5,7-dihydroxy-3,4-dimethoxyflavone, which occupies the specificity pocket S1 of the enzyme and in the same time binds to the catalytic site serine residue, which makes it a perfect potential inhibitor for trypsin-like serine proteases. In addition, in comparison with the docking output of benzamidine, amentoflavone, 5,7-dihydroxy-3,4-dimethoxyflavone, and quercetin3-O-sophoroside-7-O-rhamnoside have been found to be more effective as inhibitors for *F. oxysporum* trypsin than benzamidine whose effectiveness as a serine protease inhibitor has been proven [34]. Several in vitro and in silico [35] studies had suggested that flavonoids could be effective inhibitors for different types of proteases including serine proteases; according to the results reported by [36], amentoflavone caused the inhibition of 50% of the cysteine protease Cathepsin B at 1.75 μ M. Furthermore, it has been reported that quercetin and amentoflavone inhibited 50% of human thrombin activity at 57.77 and 19.5 μ M, respectively [37].

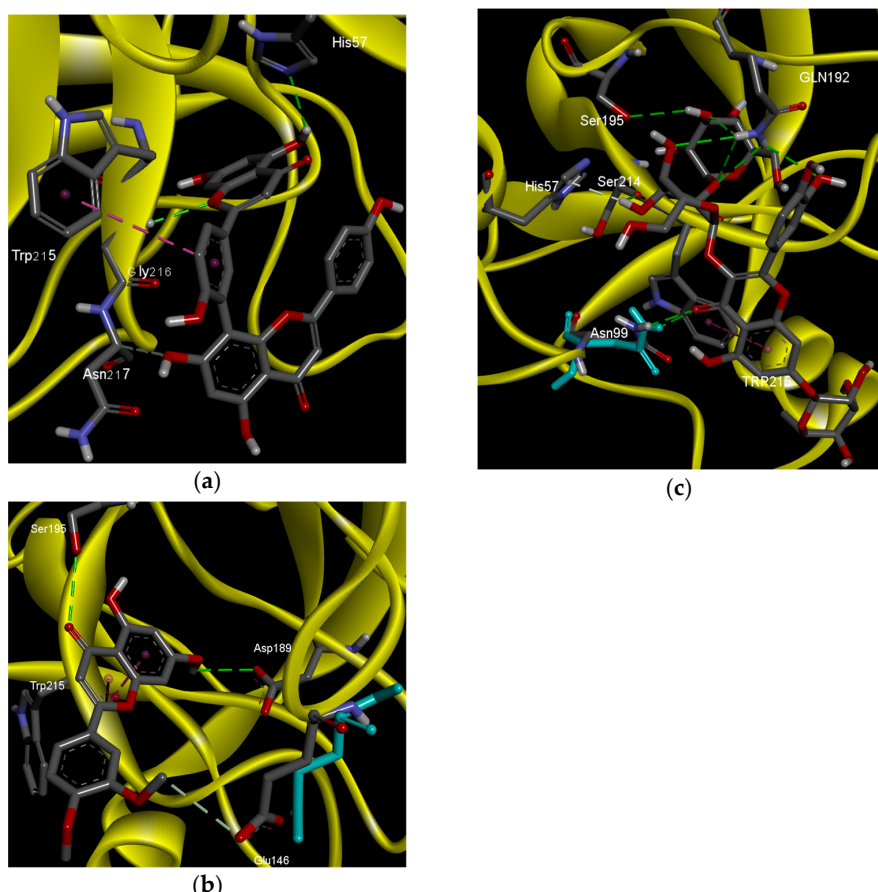


Figure 6. 3D interactions of (a) amentoflavone; (b) 5,7-Dihydroxy-3,4-dimethoxyflavone; (c) quercetin3-O-sophoroside-7-O-rhamnoside with *F. oxysporum* trypsin. Hydrogen bonds in green dashes, carbon hydrogen bonds in light green dashes, hydrophobic interactions in magenta dashes, the interacted residues and ligands in gray sticks, and the enzyme in yellow cartoon.

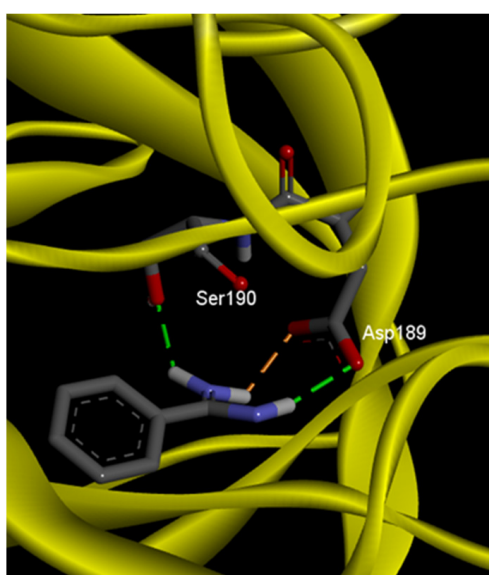


Figure 7. 3D interactions of benzamidine with *F. oxysporum* trypsin. Hydrogen bonds in green dashes, salt bridge in orange dashes, the interacted residues and ligands in gray sticks, and the enzyme in yellow cartoon.

Borapetoside A binds to the active site via two hydrogen bonds with Gly216, a hydrophobic interaction (Pi–Pi T-shaped) with His57, and van der Waals forces with Ser195, Gly219, and Asn217 in the active site of the enzyme, and binds to four residues outside the active site Asn99 via a hydrogen bond, Cys42 and Trp41 via hydrophobic interactions, Pi alkyl and Pi–Pi T-shaped, respectively, and Gln192 via an unfavorable interaction (unfavorable acceptor–acceptor); however, Borapetoside A showed the lowest affinity toward the enzyme active site. The low binding energy was attributed to the unfavorable interaction with the Gln192 residue outside the active site of the enzyme. Despite the relatively low binding energy, the result of the docking suggests that Borapetoside A could be a potential inhibitor for the *F. oxysporum* trypsin-like serine protease. The inhibitory effect of diterpenoids and their derivatives against the serine protease has been reported [38].

Plumbagin was the only compound that does not bind to the catalytic site or the specificity pocket of the enzyme through hydrogen bonds or hydrophobic interactions but interacts with a relatively high affinity with two residues in the specificity pocket, Gly216 and Asn217, and four residues outside the active site of the enzyme, Asn99, Trp215, Try172, and Ala175. It is unknown whether plumbagin interactions would affect the enzyme activity or not.

3. Materials and Methods

3.1. Materials

Black cumin seeds (*Nigella sativa*) were purchased from Ragab El Attar herbs shop at Cairo, Egypt. All the solvents utilized in the current study were of analytical grade and purchased from Sigma-Aldrich, Cairo, Egypt.

3.2. Preparation of Extract

Black cumin seeds were ground to fine powder and extracted using step-wise extraction technique. The ground seeds were extracted by macerating 50 gm of the resulted powder in 500 mL of solvent and hexane, followed by methylene chloride, and then methanol 70% (*v/v*) was prepared as 70 parts of absolute methanol to 30 parts of distilled water at room temperature (28 °C). Every step of the extraction was repeated 3 times. The extracts were recovered from solvents by air drying the solvents at room temperature (28 °C) [39].

3.3. High-Pressure Liquid Chromatography–Mass Spectrometry (HPLC-MS) Analysis

Chemical composition of black cumin seeds' methanolic extract was determined by HPLC-MS. Shimadzu HPLC-2040 (Shimadzu, Kyoto, Japan) equipped with LC 2024 controller, LC-2040 Pump, LC-2040 autosampler, and LC2030/2040 PDA detector at 254 nm was used. Shimadzu uplcms 8045 C-18 column (1.7 mm × 2.1 mm × 50 mm) was used for compound separation, and Bruker triple quadrupole LC-mass spectrometer was employed. The mobile phase was gradient of water and acetonitrile, ranging from 5% acetonitrile to 95% at flow rate of 0.2 mL/min, and the injected volume was 2 μ L. The interface was set to 4.00 kv voltage and 300 °C temperature, and the flow rate of the heating and drying gases were 10.00 L/min. Negative electrospray ionization mood was used and the mass spectra were recorded at 3000 u/s scan speed in the range of 100–1200 m/z . The compounds were identified by comparing the resulting spectrums with WILEY 09 and NIST 11 mass spectral databases and literature, and the structure of identified compounds was drawn using King Draw 3.0 software (King Draw Business Corporation, Qingdao, China).

3.4. Ligand Preparation

Ligand structure was drawn using Chem Draw 21.0.0 (PerkinElmer, Waltham, MA, USA) and saved as SDF files. Ligand energy was minimized by MM2 calculation, logP was calculated, and the structures of the ligands were converted to pdb file format using Chem3D 21.0.0. Nonpolar hydrogen atoms were deleted, Gasteiger charges were calculated, torsion root was detected, and the structures were saved as pdbqt file format using AutoDockTools-1.5.6.

3.5. Target Protein Preparation

The target protein, *Fusarium Oxysporum* trypsin-like serine protease enzyme structure encoding 1GDN [4], was downloaded from Protein Data Bank "www.rcsb.org/" (accessed on 24 July 2022)". The target protein structure was prepared by deleting water and solvent molecules and ligands, adding polar hydrogen atoms, calculating kollman charges, and saving the structure of target protein as pdbqt using AutoDockTools-1.5.6 (The Scripps Research Institute, San Diego, CA, USA).

3.6. Molecular Docking Procedures

The molecular interactions between the active site of *Fusarium oxysporum* trypsin-like serine protease and eight compounds of black cumin seeds' methanolic extract and the known serine protease inhibitor, benzamidine, were determined using AutoDock Vina 1.2.0 (The Scripps Research Institute, San Diego, CA, USA) [40]. A random seed number was used and the exhaustiveness function was increased to 32. A 18 × 15 × 22 Å grid box with 2.663 × −1.211 × −9.636 grid point spacing of 1 Å was used for docking the ligand into the enzyme active site.

3.7. Analysis and Visualization of Protein–Ligand Interactions

The conformers of each ligand were separated using vina_split command. The conformer with the highest affinity was analyzed and visualized using Discovery Studio-21 software (Dassault Systems BIOVIA San Diego, CA, USA). In silico interactions between the substrate and *F. oxysporum* trypsin-like serine protease was analyzed and visualized using PyMOL software (Schrödinger, Inc., Broadway, NY, USA).

4. Conclusions

The HPLC-MS analysis clearly indicated that black cumin seeds' methanolic extract consists mainly of flavonoids, triterpenes glycosides, diterpene glycosides, and phenolic compounds. Amentoflavone, Procyanidin C2, Quercetin3-O-sophoroside-7-O-rhamnoside, 5,7-Dihydroxy-3,4-dimethoxyflavone, Borapetoside A, tetrahydroxy-urs-12-en-28-O-[β -D-glucopyranosyl (1-2)- β -D-glucopyranosyl] ester, and kudzusaponogenol A-hexA-pen are the major compounds. The molecular docking results showed that amentoflavone,

5,7-dihydroxy-3,4-dimethoxyflavone, and quercetin3-O-sophoroside-7-O-rhamnoside are effectively able to inhibit *F. oxysporum* trypsin. This suggests that black cumin seeds' methanolic extract is a source for potential trypsin-like serine protease inhibitors. Our results support the use of black cumin seeds' methanolic extract as a natural eco-friendly fungicide against the diseases caused by *F. oxysporum*. Although it has been proven that molecular docking is a very useful tool in structure-based drug discovery, further in vitro studies are needed to confirm the inhibitory effect of amentoflavone, 5,7-dihydroxy-3,4-dimethoxyflavone, and quercetin3-O-sophoroside-7-O-rhamnoside.

Author Contributions: Conceptualization, H.S.E.-B., S.M.S.A.A., A.I.A., M.A.R.I., M.F.M.I., M.A.A., D.B.E.D., S.M.A.-Q., N.A.A.-H., H.D. and H.A.M.S.; data curation, D.B.E.D., S.M.A.-Q., N.A.A.-H. and H.A.M.S.; formal analysis, H.S.E.-B., S.M.S.A.A., A.I.A., M.A.R.I., M.F.M.I., M.A.A. and H.D.; funding acquisition, H.S.E.-B.; investigation, H.S.E.-B., M.F.M.I. and H.A.M.S.; methodology, S.M.S.A.A., A.I.A., M.A.R.I. and H.A.M.S.; project administration, H.S.E.-B., M.F.M.I. and H.A.M.S.; resources, M.A.A., D.B.E.D., S.M.A.-Q., N.A.A.-H., H.D. and H.A.M.S.; software, S.M.S.A.A., A.I.A., M.A.R.I., M.F.M.I., M.A.A. and H.A.M.S.; supervision, H.S.E.-B., M.F.M.I. and H.A.M.S.; validation, H.S.E.-B., S.M.S.A.A., A.I.A., M.A.R.I., M.F.M.I., M.A.A., D.B.E.D., S.M.A.-Q., N.A.A.-H. and H.A.M.S.; visualization, H.S.E.-B., S.M.S.A.A., A.I.A., M.A.R.I., M.F.M.I., M.A.A., D.B.E.D., S.M.A.-Q., N.A.A.-H., H.D. and H.A.M.S.; writing—original draft, S.M.S.A.A., A.I.A., M.A.R.I. and H.A.M.S.; writing—review & editing, H.S.E.-B., S.M.S.A.A., A.I.A., M.A.R.I., M.F.M.I., M.A.A., D.B.E.D., S.M.A.-Q., N.A.A.-H., H.D. and H.A.M.S. All authors have read and agreed to the published version of the manuscript.

Funding: This work was supported by the Deanship of Scientific Research, Vice Presidency for Graduate Studies and Scientific Research, King Faisal University, Saudi Arabia (GRANT 3202).

Institutional Review Board Statement: Not applicable.

Informed Consent Statement: Not applicable.

Data Availability Statement: All data are available within the manuscript.

Acknowledgments: The authors are thankful to the Deanship of Scientific Research, Vice Presidency for Graduate Studies and Scientific Research, King Faisal University, Saudi Arabia, for supporting this research work.

Conflicts of Interest: The authors declare no conflict of interest.

References

- El-Abyad, M.S.; Abu-Taleb, A.M.; Abdel-Mawgoud, T. Response of host cultivar to cell wall-degrading enzymes of the sugarbeet pathogens *Rhizoctonia solani* Kühn and *Sclerotium rolfsii* Sacc. under salinity stress. *Microbiol. Res.* **1997**, *152*, 9–17. [[CrossRef](#)]
- Gvozdeva, E.L.; Volotskaya, A.V.; Sof'in, A.V.; Kudryavtseva, N.N.; Revina, T.A.; Valueva, T.A. Interaction of proteinases secreted by the fungal plant pathogen *Rhizoctonia solani* with natural proteinase inhibitors produced by plants. *Appl. Biochem. Microbiol.* **2006**, *42*, 502–507. [[CrossRef](#)]
- Ekici, Ö.D.; Paetzl, M.; Dalbey, R.E. Unconventional serine proteases: Variations on the catalytic Ser/His/Asp triad configuration. *Protein Sci.* **2008**, *17*, 2023–2037. [[CrossRef](#)]
- Rypniewski, W.R.; Østergaard, P.R.; Nørregaard-Madsen, M.; Dauter, M.; Wilson, K.S. *Fusarium oxysporum* trypsin at atomic resolution at 100 and 283 K: A study of ligand binding. *Acta Crystallogr. Sect. D Biol. Crystallogr.* **2001**, *57*, 8–19. [[CrossRef](#)]
- Abd-El-Khair, H.; El-Gamal, N.G. Effects of aqueous extracts of some plant species against *Fusarium solani* and *Rhizoctonia solani* in *Phaseolus vulgaris* plants. *Arch. Phytopathol. Plant Prot.* **2011**, *44*, 1–16. [[CrossRef](#)]
- Marei, G.I.K.; Abdelgaleil, S.A.M. Antifungal potential and biochemical effects of monoterpenes and phenylpropenes on plant. *Plant Prot. Sci.* **2018**, *54*, 9–16. [[CrossRef](#)]
- Hamza, A.; Mohamed, A.; Derbalah, A. Unconventional alternatives for control of tomato root rot caused by *Rhizoctonia solani* under greenhouse conditions. *J. Plant Prot. Res.* **2016**, *56*, 298–305. [[CrossRef](#)]
- Aftab, A.; Yousaf, Y.; Javaid, A.; Riaz, N.; Younas, A.; Rashid, M.; Shamsher, B.; Arif, A. Antifungal activity of vegetative methanolic extracts of *Nigella sativa* against *Fusarium oxysporum* and *Macrophomina phaseolina* and its phytochemical profiling by GC-MS analysis. *Int. J. Agric. Biol.* **2019**, *21*, 569–576.
- Kadam, D.; Lele, S.S. Extraction, characterization and bioactive properties of *Nigella sativa* seedcake. *J. Food Sci. Technol.* **2017**, *54*, 3936–3947. [[CrossRef](#)] [[PubMed](#)]
- Soleimanifar, M.; Niazmand, R.; Jafari, S.M. Evaluation of oxidative stability, fatty acid profile, and antioxidant properties of black cumin seed oil and extract. *J. Food Meas. Charact.* **2019**, *13*, 383–389. [[CrossRef](#)]

11. Muthu Kumara, S.S.; Kwong Huat, B.T. Extraction, Isolation and Characterisation of Antitumor Principle, α -Hederin, from the Seeds of *Nigella sativa*. *Planta Med.* **2001**, *67*, 29–32. [[CrossRef](#)]
12. Ahmad, A.; Husain, A.; Mujeeb, M.; Alam Khan, S.; Najmi, A.K.; Siddique, N.A.; Damanhouri, Z.A.; Anwar, F. A review on therapeutic potential of *Nigella sativa*: A miracle herb. *Asian Pac. J. Trop. Biomed.* **2013**, *3*, 337–352. [[CrossRef](#)]
13. Chaieb, K.; Kouidhi, B.; Jrah, H.; Mahdouani, K.; Bakhouf, A. Antibacterial activity of Thymoquinone, an active principle of *Nigella sativa* and its potency to prevent bacterial biofilm formation. *BMC Complement. Altern. Med.* **2011**, *11*, 29. [[CrossRef](#)]
14. Bordoni, L.; Fedeli, D.; Nasuti, C.; Maggi, F.; Papa, F.; Wabitsch, M.; De Caterina, R.; Gabbianelli, R. Antioxidant and Anti-Inflammatory Properties of *Nigella sativa* Oil in Human Pre-Adipocytes. *Antioxidants* **2019**, *8*, 51. [[CrossRef](#)]
15. El Aziz, S.M.S.A.; Abo-Shady, A.; Ibrahim, M.; Helmy, M.M. Inhibition of *Rhizoctonia solani* Growth and Its Extracellular Hydrolytic Enzymes by Different Extracts of Cinnamon (*Cinnamomum cassia*) and Black Cumin Seeds (*Nigella sativa*). *Arab. Univ. J. Agric. Sci.* **2022**, *30*, 1–18. [[CrossRef](#)]
16. Li, H.; DaSilva, N.A.; Liu, W.; Xu, J.; Dombi, G.W.; Dain, J.A.; Li, D.; Chamcheu, J.C.; Seeram, N.P.; Ma, H. Thymocid®, a Standardized Black Cumin (*Nigella sativa*) Seed Extract, Modulates Collagen Cross-Linking, Collagenase and Elastase Activities, and Melanogenesis in Murine B16F10 Melanoma Cells. *Nutrients* **2020**, *12*, 2146. [[CrossRef](#)] [[PubMed](#)]
17. Morris, G.M.; Marguerita, L.-W. Molecular docking. In *Molecular Modeling of Proteins*, 1st ed.; Kukol, A., Ed.; Humana: Totowa, NJ, USA, 2008; pp. 365–382. [[CrossRef](#)]
18. Yao, H.; Chen, B.; Zhang, Y.; Ou, H.; Li, Y.; Li, S.; Shi, P.; Lin, X. Analysis of the Total Biflavonoids Extract from *Selaginella doederleinii* by HPLC-QTOF-MS and Its In Vitro and In Vivo Anticancer Effects. *Molecules* **2017**, *22*, 325. [[CrossRef](#)] [[PubMed](#)]
19. Enomoto, H.; Takahashi, S.; Takeda, S.; Hatta, H. Distribution of Flavan-3-ol Species in Ripe Strawberry Fruit Revealed by Matrix-Assisted Laser Desorption/Ionization-Mass Spectrometry Imaging. *Molecules* **2019**, *25*, 103. [[CrossRef](#)] [[PubMed](#)]
20. Tsugawa, H.; Nakabayashi, R.; Mori, T.; Yamada, Y.; Takahashi, M.; Rai, A.; Sugiyama, R.; Yamamoto, H.; Nakaya, T.; Yamazaki, M.; et al. A cheminformatics approach to characterize metabolomes in stable-isotope-labeled organisms. *Nat. Methods* **2019**, *16*, 295–298. [[CrossRef](#)]
21. Fabre, N.; Rustan, I.; de Hoffmann, E.; Quetin-Leclercq, J. Determination of flavone, flavonol, and flavanone aglycones by negative ion liquid chromatography electrospray ion trap mass spectrometry. *J. Am. Soc. Mass Spectrom.* **2001**, *12*, 707–715. [[CrossRef](#)]
22. Lewars, E.G.; March, R.E. Fragmentation of 3-hydroxyflavone; a computational and mass spectrometric study. *Rapid Commun. Mass Spectrom.* **2007**, *21*, 1669–1679. [[CrossRef](#)]
23. Benayad, Z.; Gómez-Cordovés, C.; Es-Safi, N.E. Characterization of Flavonoid Glycosides from Fenugreek (*Trigonella foenum-graecum*) Crude Seeds by HPLC–DAD–ESI/MS Analysis. *Int. J. Mol. Sci.* **2014**, *15*, 20668–20685. [[CrossRef](#)] [[PubMed](#)]
24. Li, Z.-H.; Guo, H.; Xu, W.-B.; Ge, J.; Li, X.; Alimu, M.; He, D.-J. Rapid Identification of Flavonoid Constituents Directly from PTP1B Inhibitive Extract of Raspberry (*Rubus idaeus* L.) Leaves by HPLC–ESI–QTOF–MS–MS. *J. Chromatogr. Sci.* **2016**, *54*, 805–810. [[CrossRef](#)]
25. Singh, A.; Bajpai, V.; Kumar, S.; Sharma, K.R.; Kumar, B. Profiling of Gallic and Ellagic Acid Derivatives in Different Plant Parts of *Terminalia arjuna* by HPLC–ESI–QTOF–MS/MS. *Nat. Prod. Commun.* **2016**, *11*, 239–244. [[CrossRef](#)]
26. Brito, A.; Ramirez, J.E.; Areche, C.; Sepúlveda, B.; Simirgiotis, M.J. HPLC–UV–MS Profiles of Phenolic Compounds and Antioxidant Activity of Fruits from Three Citrus Species Consumed in Northern Chile. *Molecules* **2014**, *19*, 17400–17421. [[CrossRef](#)] [[PubMed](#)]
27. Nascimento, Y.M.; Abreu, L.S.; Lima, R.L.; Costa, V.C.O.; de Melo, J.I.M.; Braz-Filho, R.; Silva, M.S.; Tavares, J.F. Rapid Characterization of Triterpene Saponins from *Zornia brasiliensis* by HPLC–ESI–MS/MS. *Molecules* **2019**, *24*, 2519. [[CrossRef](#)]
28. Wang, H.-Y.; Liu, K.; Wang, R.-X.; Qin, S.-H.; Wang, F.-L.; Sun, J.-Y. Two new triterpenoids from *Nauclea officinalis*. *Nat. Prod. Res.* **2015**, *29*, 644–649. [[CrossRef](#)] [[PubMed](#)]
29. Mad, T.; Sterk, H.; Mittelbach, M.; Rechberger, G.N. Tandem mass spectrometric analysis of a complex triterpene saponin mixture of *Chenopodium quinoa*. *J. Am. Soc. Mass Spectrom.* **2006**, *17*, 795–806. [[CrossRef](#)]
30. Xu, L.-L.; Guo, F.-X.; Chi, S.-S.; Wang, Z.-J.; Jiang, Y.-Y.; Liu, B.; Zhang, J.-Y. Rapid Screening and Identification of Diterpenoids in *Tinospora sinensis* Based on High-Performance Liquid Chromatography Coupled with Linear Ion Trap–Orbitrap Mass Spectrometry. *Molecules* **2017**, *22*, 912. [[CrossRef](#)]
31. Hassan, W.H.B.; Abdelaziz, S.; Al Yousef, H.M. Chemical Composition and Biological Activities of the Aqueous Fraction of *Parkinsonia aculeata* L. Growing in Saudi Arabia. *Arab. J. Chem.* **2019**, *12*, 377–387. [[CrossRef](#)]
32. Fischer, U.A.; Carle, R.; Kammerer, D.R. Identification and quantification of phenolic compounds from pomegranate (*Punica granatum* L.) peel, mesocarp, aril and differently produced juices by HPLC–DAD–ESI/MSn. *Food Chem.* **2011**, *127*, 807–821. [[CrossRef](#)]
33. Hsieh, Y.-J.; Lin, L.-C.; Tsai, T.-H. Determination and identification of plumbagin from the roots of *Plumbago zeylanica* L. by liquid chromatography with tandem mass spectrometry. *J. Chromatogr. A* **2005**, *1083*, 141–145. [[CrossRef](#)] [[PubMed](#)]
34. Steinmetzer, T.; Hardes, K. The antiviral potential of host protease inhibitors, in Activation of Viruses by Host Proteases. *Act. Viruses Host Proteases* **2018**, *16*, 279–325. [[CrossRef](#)]
35. Selim, S.; Almuhayawi, M.S.; Alharbi, M.T.; Al Jaouni, S.K.; Alharthi, A.; Abdel-Wahab, B.A.; Ibrahim, M.A.R.; Alsuhaimani, A.M.; Warrad, M.; Rashed, K. Insights into the Antimicrobial, Antioxidant, Anti-SARS-CoV-2 and Cytotoxic Activities of *Pistacia lentiscus* Bark and Phytochemical Profile; In Silico and In Vitro Study. *Antioxidants* **2022**, *11*, 930. [[CrossRef](#)]
36. Pan, X.; Tan, N.; Zeng, G.; Zhang, Y.; Jia, R. Amentoflavone and its derivatives as novel natural inhibitors of human Cathepsin B. *Bioorgan. Med. Chem.* **2005**, *13*, 5819–5825. [[CrossRef](#)] [[PubMed](#)]

37. Wei, L.-H.; Chen, T.-R.; Fang, H.-B.; Jin, Q.; Zhang, S.-J.; Hou, J.; Yu, Y.; Dou, T.-Y.; Cao, Y.-F.; Guo, W.-Z.; et al. Natural constituents of St. John's Wort inhibit the proteolytic activity of human thrombin. *Int. J. Biol. Macromol.* **2019**, *134*, 622–630. [[CrossRef](#)] [[PubMed](#)]
38. Khan, R.A.; Hossain, R.; Siyadatpanah, A.; Al-Khafaji, K.; Khalipha, A.B.R.; Dey, D.; Asha, U.H.; Biswas, P.; Saikat, A.S.M.; Chenari, H.A.; et al. Diterpenes/Diterpenoids and Their Derivatives as Potential Bioactive Leads against Dengue Virus: A Computational and Network Pharmacology Study. *Molecules* **2021**, *26*, 6821. [[CrossRef](#)] [[PubMed](#)]
39. Abubakar, A.; Haque, M. Preparation of medicinal plants: Basic extraction and fractionation procedures for experimental purposes. *J. Pharm. Bioallied Sci.* **2020**, *12*, 1–10. [[CrossRef](#)]
40. Eberhardt, J.; Santos-Martins, D.; Tillack, A.F.; Forli, S. AutoDock Vina 1.2.0: New Docking Methods, Expanded Force Field, and Python Bindings. *J. Chem. Inf. Model.* **2021**, *61*, 3891–3898. [[CrossRef](#)]

Disclaimer/Publisher's Note: The statements, opinions and data contained in all publications are solely those of the individual author(s) and contributor(s) and not of MDPI and/or the editor(s). MDPI and/or the editor(s) disclaim responsibility for any injury to people or property resulting from any ideas, methods, instructions or products referred to in the content.